JOURNAL OF IRON AND STEEL RESEARCH, INTERNATIONAL. 2010, 17(10): 50-56

Ultrafine Grained HSLA Steels for Cold Forming

R González[1], J O García[2], M A Barbés[2], M J Quintana[1], L F Verdeja[2], J I Verdeja[2]
(1. School of Engineering, Panamerican University, Mexico City 03920, Mexico;
2. ETSIMO, Oviedo University, Oviedo 33004, Asturias, Spain)

Abstract: The industrial level production of ultrafine grained (or ultrafine ferrite) ferrous alloys was investigated through three examples of steels that complied with the EN 10149-2 Euronorm and were produced by advanced controlled hot rolling techniques. The steel samples were tension tested and chemically analyzed, and the microstructure was evaluated through quantitative metallographic techniques to determine parameters such as yield stress, amount of microalloying elements, strain hardening coefficient, grain size, and grain size distribution. These steels were microalloyed with Ti, Nb, and Mn with ASTM grain sizes of approximately 13－15. The careful control of chemical composition and deformation during production, giving a specific attention to the deformation sequences, austenite nonrecrystallization temperatures and allotropic transformations during cooling, are indispensable to obtain steels with an adequate strain hardening coefficient that allows cold working operations such as bending, stretching or drawing.
Key words: ultrafine steel; metallography; strain hardening; Euronorm

Though the most important industries for the 21st century are thought to be the development of advanced materials (also known as new materials), information technologies, artificial intelligence, and biotechnology[1], price reductions and improvements in quality and properties in steel have maintained this material as a leader in all industrial applications[2]. More specifically, the use of structural materials in the second half of the 20th century included the competition between Fe-C alloys and other metallic materials, which resulted in advanced steels that respond to large production necessities. The interest in Fe alloys is based upon other things, in its changes during solid state transformations, restoration and recrystallization, and textures[3].

For example, there is an ongoing activity in the steel industry to develop new methods to produce high strength low alloy (HSLA) structural steels with lower cost and improved properties. The use of heat treatments such as normalizing and quenching and tempering, and more recently, thermomechanical controlled rolling processing techniques (TMCRP) and the use of continuous annealing processing lines (CAPL) have been developed to produce fine ferrite grain sizes in final products. These techniques have shown a significant improvement in strength, fracture toughness, and weldability through the refinement of ferrite grain size (up to 12 ASTM G, $d_\alpha \approx 5$ μm), which was the grain size lower limit reachable in the industry 30 years ago[4]. However, the Hall-Petch equation predicts that a reduction from 5 to 1 μm should increase the yield strength of a given steel up to 350 MPa and decrease the impact transition temperature (ITT) up to −100 ℃[5]. In this study, the results of current commercial techniques like TMCRP are presented, which improve properties and allow the replacement of some costly alloy steels with either plain carbon or microalloyed/low alloyed carbon steels, demonstrating that the industrial production of fine, equiaxed ferrite grains with $d \approx 2-3$ μm is possible.

Thermomechanical processing such as controlled rolling, controlled cooling and direct quenching save energy in steel manufacture by minimizing or even eliminating the heat treatment after hot deformation, thereby increasing the productivity for high grade steels. It generally demands a change in alloy design and frequently reduces the productivity of the hot deformation process itself, but makes it possible to reduce the total amount of alloying addi-

Biography: R González(1967—), Male, Doctor; **E-mail**: robglez@up.edu.mx; **Received Date**: October 20, 2009

tions and to improve strength, toughness, and weldability, whilst sometimes producing new and beneficial characteristics in the steel.

A large amount of the rolled steel products currently produced are of the microalloyed type. These steels are usually soaked at high temperatures when roughing deformation is carried out. In the case of conventional controlled rolling (CCR), rough rolling is followed by fast cooling and finishing passes are carried out at temperatures where the austenite remains un-recrystallized. The microalloying elements, which remain in solution (partially or completely) during rough deformation, start to precipitate after finishing deformations at low temperatures. Nb, Ti and V are the most commonly used microalloying elements and during cooling, they combine with C and/or N to form carbide, nitride and/or carbonitride precipitates. These fine precipitates play an effective role by retarding recrystallization (and therefore, increasing the recrystallization-stop temperature) that usually follows deformation and thus, helps to retain the accumulated strain and deformed structures of austenite grains.

1 Experimental

The research was made in three HSLA steels in the form of sheet with different thicknesses, obtained by TMCRP in its raw hot rolled state: S355 (4.5 mm), S460 (5 mm) and S550 (3.5 mm). The chemical composition and mechanical properties established by the EN 10149-2 (1995) Euronorm are presented in Table 1 and Table 2, whereas the chemical analysis of the hot rolled strip in mass percent is given in Table 3. The values for C and S were analyzed in an LECO CS444 system by the combustion method; for the remaining elements, an ARL 4460 optical emission spectrometer was used, and Table 3 indicates the average of three measurements.

To determine hardness, tests were made following the UNE-EN IS06507-1 standard, which specifies the Vickers scale (HV). A GNEHM OM-150 universal model durometer was used with a load of 100 N, and the results, average of five measurements in each sample (in the rolling plane surface), are presented in Table 4.

Tension and resilience properties were evaluated by machining samples from the strip with a calibrated length of 100 mm, a gauge of 50 mm, width of 10 mm and thickness of 3 mm, in accordance to UNE-EN 10002-1 standard. The samples were tested in an INSTRON 1195 universal machine, equipped with a load cell of 100 kN. Engineering yield stress,

Table 1 Chemical composition of thermomechanically rolled steels

Name	Material number	w_C/%	w_{Mn}/%	w_{Si}/%	w_P/%	w_S/%[1]	w_{Alt}/%	w_{Nb}/%[2]	w_V/%[2]	w_{Ti}/%[2]	w_{Mo}/%	w_B/%
S355	1.0976	≤0.12	≤1.50	≤0.50	≤0.025	≤0.020	≥0.015	≤0.09	≤0.20	≤0.15	—	—
S460	1.0982	≤0.12	≤1.60	≤0.50	≤0.025	≤0.015	≥0.015	≤0.09	≤0.20	≤0.15	—	—
S550	1.0986	≤0.12	≤1.80	≤0.50	≤0.025	≤0.015	≥0.015	≤0.09	≤0.20	≤0.15	—	—

Note: 1) If ordered, the sulphur content should be less than 0.01%; 2) The sum of Nb, V and Ti should be less than 0.22%.

Table 2 Mechanical properties for thermomechanically rolled steels

Name	Material number	Minimum yield strength/MPa	Tensile strength/MPa[1]	Minimum percentage elongation at fracture		Minimum mandrel diameter when bending at 180°
				If $t<3$ mm, $L_0=80$ mm[2]	If $t\geqslant 3$ mm, $L_0=5.65\sqrt{S_0}$[3]	
S355	1.0976	355	430—550	19	23	0.5t
S460	1.0982	460	520—670	14	17	1t
S550	1.0986	550	600—760	12	14	1.5t

Note: 1) The values for the tensile and bending tests apply to longitudinal test pieces and transverse test pieces, respectively; For thickness $t>8$ mm, the minimum yield strength can be 20 MPa lower; 2) L_0 is the initial length of the tension test sample; 3) S_0 is the initial width of the tension test sample.

Table 3 Chemical composition of investigated steels (mass percent, %)

Steel	C	Si	Mn	P	S	Al	Ti	Nb	V	Cu	N
S355	0.06	0.01	0.32	0.011	0.009	0.026	0.002	0.023	—	0.015	0.056
S460	0.07	0.01	0.60	0.009	0.013	0.036	0.062	0.043	—	0.016	0.042
S550	0.07	0.19	1.55	0.016	0.004	0.029	0.070	0.048	0.005	—	0.045

Table 4 Mechanical properties of investigated steels

Steel	S355	S460	S550
HV10	160	181	220
Equivalent ultimate tensile strength from hardness/MPa	553	607	710
Yield strength/MPa	405	532	630
Ultimate tensile strength/MPa	549	603	711
Total elongation/%	34	22	21
Yield strength/Ultimate tensile strength	0.74	0.88	0.89
Strain hardening coefficient	0.13	0.12	0.11

engineering ultimate tensile strength and total elongation were measured and the ASTM E-646-78 standard was used to determine the tensile strain hardening coefficient n, from the engineering stress (s) -strain (e) curve (Fig. 1), using the Ludwik-Hollomon power curve mathematical expression $\sigma = K\varepsilon^n$, where σ, ε are the true stress and the true strain, respectively, and K is a constant.

Metallographic characterization was carried out on the transverse section parallel to the rolling direction, after mechanical grinding, 6 and 1 μm diamond paste polishing and final polishing with 0.05 μm γ-alumina solution. The Nital-2 reactive was used to etch the samples, which were observed in a Nikon-Epiphot metallographic optical microscope. Due to the fact that in all cases, magnifications higher than 100 were used (as these are ultrafine ferrite steels-UFF, qualitative determination of the ASTM G number, was made using the formula[6]:

$$G = G' + 6.64 \cdot \lg \frac{M}{100} \quad (1)$$

where, G' is the ASTM grain size measured as if the micrograph was taken at a magnification of 100; and M is the actual magnification of the micrograph.

For quantitative metallographic analysis of grain size (mean linear intercept) and volume fraction of the minority constituents (pearlite), a Buehler Omnimet image analyzer system connected to the Nikon Epiphot microscope was used, in accordance to the ASTM E112 standard and the expanded version E1181-02. The measurement of the mean linear intercept is automatically performed by the equipment on lines traced on the micrograph at 0°, 45°, 90° and 135° from the rolling direction. Volume fraction f_v of the pearlite phase is measured by point counting analysis on the micrographs using a mesh of dots with an optimal gap in order to avoid that two consecutive dots are placed in the same pearlite colony. The number of dots measured was at least 396, which results in $f_v/\sigma_v = 0.05$, where σ_v is the standard deviation in statistical analysis, resulting in a confidence level of 95% for the pearlite volume fraction[7]. The relationship between ASTM G grain size and the mean linear intercept $\bar{L}$, in the case of the ferrite phase, was calculated with the formula:

$$G = -3.356 - 6.644 \lg \bar{L} \quad (2)$$

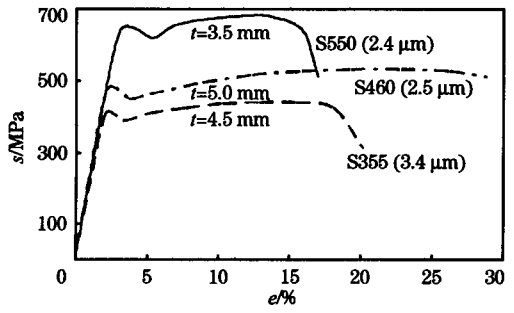

Fig. 1 Engineering stress-strain curves for investigated steels

2 Results and Discussion

The micrographs taken from transverse sections parallel to the rolling direction of S355, S460 and S550 steels show common characteristics (Fig. 2): slight banding of the microstructure in the rolling direction, pancake structure of the ferrite caused by the controlled rolling process with elongated grains in the rolling direction, totally recrystallized structures, and very small volume fraction of pearlite.

The grain morphology in S355 [Fig. 2 (a)] is considerably different from those of samples S460 and S550 [Fig. 2 (b) and (c)], as the latter two steel samples show evidently elongated grains, which also explain their higher yield strength and ultimate tensile strength (Table 4), regardless of the sheet thickness. In Table 4, the estimated ultimate tensile strength values obtained from the hardness are also compared with the tension test ones, resulting in very similar numbers.

Fig. 3 presents the ASTM G grain size frequency histograms for three typical sets of micrographs of the investigated steels, resulting in the data for $\bar{G}$, sd standard deviation and $\bar{L}$ indicated in Table 5. It is clear that these are UFF steels with $\bar{L}$ of approximately 1.9 μm for S460 and S550, and a slightly higher value (approximately 3.1 μm) for the Nb microalloyed S355. The grain size distribution is very similar in samples S460 and S550 [Fig. 3 (b) and (c)], whereas sample S355 shows a more symmetrical and wider distribution [Fig. 3 (a)], which results in a larger amount of small grains in S460 and S550, and

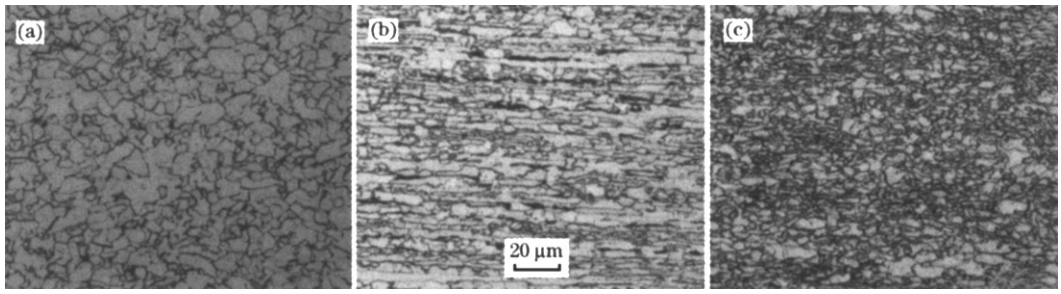

Fig. 2 Captured image of S355 steel (a), S460 steel (b), and S550 steel (c)

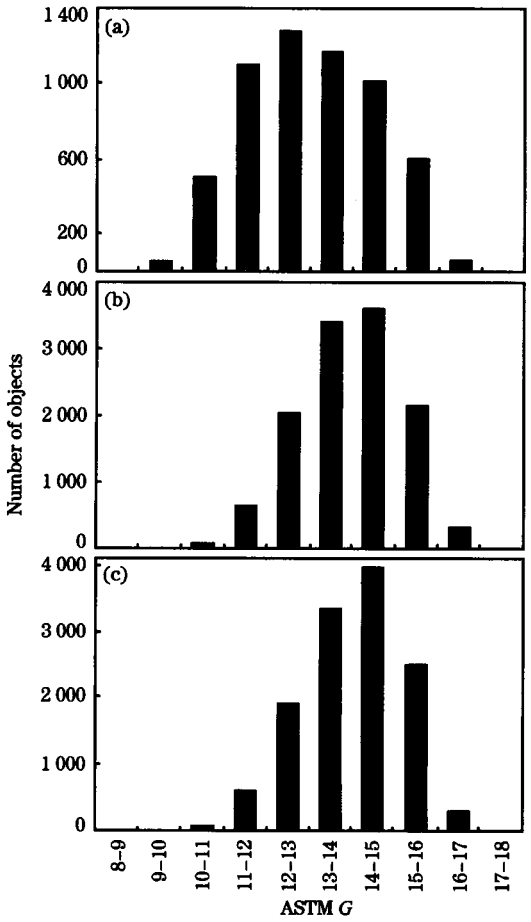

Fig. 3 ASTM grain size distribution in S355 steel (a), S460 steel (b), and S550 steel (c)

therefore a higher yield stress as indicated in Table 4, independently from the amount of second phase particles enhancing resistance.

Table 5 presents the fraction volume of pearlite and the qualitative estimate of the ASTM G grain size obtained by patterns, in accordance to the ASTM E-112 standard, in micrographs with magnification over 600.

In recent years, several reports have been presented for UFF steels, in an attempt to develop high strength along with high fracture toughness materials[8-11]. In a recent work at the Max Planck Institute[2], ultrafine grains of 1 — 2 μm were achieved in plain carbon steels by combining a hot deformation stage, followed by a heavy warm deformation and final controlled cooling. The carbon content of the steels examined ranged from 0.17% to 0.31% so that a fine cementite dispersion could be achieved in the ferrite matrix which helped to stabilize the ultrafine grains particularly during the long high temperature period while cooling. These materials resulted in yield strength of 590 MPa, ultimate tensile strength of 660 MPa, and elongation of 19%.

Table 5 Microstructural measurements for three investigated steels

Steel	S355	S460	S550
f_v of pearlite/%	3.9	6.9	2.4
ASTM G[1)]	13.0—13.5	14.5—15.0	14.5—15.0
ASTM $\bar{G}$[2)]	13.32	14.70	14.75
sd[2)]	1.67	1.54	1.63
$\bar{L}$[2)]	3.09	1.92	1.88

Note: 1) Qualitatively estimated value; 2) Values measured using the image analyzer system.

The techniques used by the authors just mentioned, ARB (accumulative roll-bonding)[8], DSIT (dynamic strain induced transformation)[9], CRA (cold rolling and annealing)[11], RTA (rapid transformation annealing)[12], are all based on some type SPD (severe plastic deformation) process. This is not the case of steels obtained by TMCRP, where the final thickness reduction (finishing) is only of 50% ($\varepsilon \approx 0.7$). Furthermore, none of these techniques have yet surpassed the laboratory level. As indicated by Howe[13], it may be deduced from all this work that UFF steels have an "Achilles' heel", as they tend to exhibit unstable plasticity upon yielding, restricting its potential industrial applica-

tions: they show uniform elongations (ε_u) and very low strain hardening coefficients ($\varepsilon_u = n < 0.1$), which makes them unviable for forming processes such as bending, stretching, and drawing at room temperature. The tensile curves for many UFF steels obtained in a laboratory scale (grain sizes as small as 0.5 μm have been reported)[12] usually show a local elongation zone normally denominated "Lüders effect" (formation of Lüders bands), which results in fracture. This behavior is typical in effervescent steels not treated with Al/Ti, and in ferrous and non-ferrous alloys with ultrafine grain size[8,14], as shown in Fig. 4 (Morrison and Miller[15], from Leslie[14]).

To explain the low ductility of the UFF steels, the results presented by Morrison and Miller[15] must be considered (Morrison law), in which n is related to the mean grain size d (equivalent to the mean linear intercept, $\bar{L}$) by the equation:

$$n=\frac{5}{10+d^{-1/2}} \tag{3}$$

results in the following: if $d=0.010$ mm, $n=0.25$ and if $d=0.0005$ mm, $n=0.09<0.1$, as shown in Fig. 5 (Morrison and Miller[15], from Leslie[14]), which means that the material has lost its capacity to strain hardening. Moreover, professor Bhadeshia[16] indicates that the apparently insatiable desire for finer microstructure has resulted in mixed outcomes in the field of structural materials: simple grain refinement leads to unacceptable poor ductility because the capacity for work-hardening is lost. Nevertheless, bulk nanostructured steels, microalloyed with Ti, Nb and V, obtained by TMCRP with good properties have been commercialized, based on its success in the $\gamma \rightarrow \alpha$ stress or strain induced transformation to

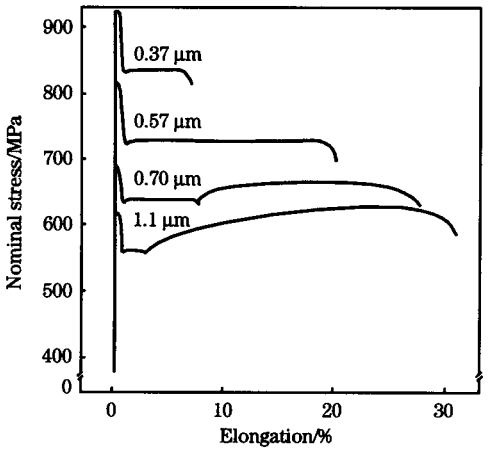

Fig. 4 Effect of grain size on elongation for tension test

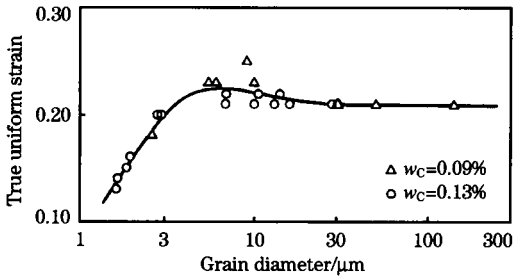

Fig. 5 Variation of uniform elongation with grain size in low-carbon steel

enhance work hardening and anisotropic grains to boost the total amount of interfaces per unit volume. This phenomena must be taken into account, as a normal very small grain size (<1 μm) in its recrystallized state loses its capacity to strain harden and has $\frac{d\sigma}{d\varepsilon}<\sigma$ and thus, if deformed, immediately shows lüdering effect and fracture without any plastic uniform deformation[17].

Fig. 6 schematically illustrates the three stages of the controlled-rolling process and the microstructural change accompanying deformation in each stage. In stage 1, coarse austenite (a) is refined by repeated deformation and recrystallization (b), though the steel transforms to relatively coarse ferrite (b'), except when using "Ti technology" which allows, before rolling is performed, the refinement of homogenized austenite grain size. During stage 2, elongated, unrecrystallized austenite deformation bands are formed (c) and ferrite nucleates on the deformation bands as well as γ-grain boundaries, resulting in fine α grains. In this case, "Nb technology" has to be used in order to accumulate deformation within the austenite when rolling happens at a temperature below the non-recrystallization temperature, T_{nr}, which is a fundamental parameter in the process. In

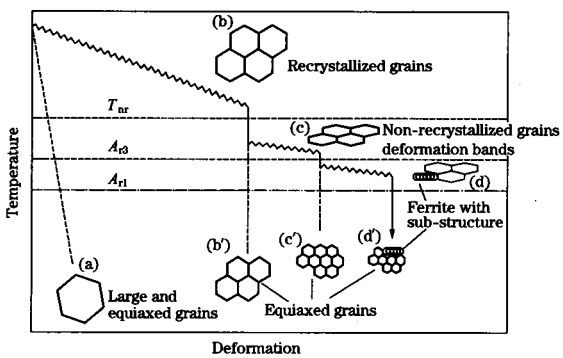

Fig. 6 Schematic diagram of controlled rolling process

the case of stage 3, deformation in the α-γ dual-phase region continues the process started in stage 2, and results in a substructure. If, in a complementary way, "V technology" is used, a structural precipitation hardening of V_4C_3 will occur in the ferrite phase.

Summarizing, controlled rolling procedures include the reduction on the rapid recrystallization region (stage 1), a delay on the rolling between stage 1 and stage 2, and a reduction in the final non-recrystallization region (stage 2). Optionally, deformation below A_{r3} (stage 3) or accelerated cooling may be followed. Accelerated cooling after hot rolling is currently being recognized as a further advanced thermomechanical treatment in the hot rolling process. This cooling process is characterized by accelerated cooling in a γ→α transformation range just after controlled rolling. It has been shown that the accelerated cooling refines the α grain size and thus further improves both the strength and toughness. In industrial practice, when fine recrystallized γ is deformed by 50% ($\varepsilon=0.7$) in the non-recrystallized region, the resulting grain size, under careful cooling conditions and coil design, is higher than 12 ASTM G ($d_\alpha<5$ μm), which compared to common normalized products with a 10 ASTM G ($d_\alpha\approx10$ μm) grain size, at their best, is a considerable improvement[18].

As indicated by Perosanz[19], the solubility products of the mentioned carbonitrides, as well as of other chemical compounds (AlN, MnS, V_4C_3), result in limit solubility temperature of the carbonitrides, non-recrystallization temperature of the austenite and γ→α allotropic transformation temperature during cooling, with values close to ($t<6$ mm):

1) Starting precipitation temperatures T_{ps}

TiN

$$\lg(w_{Ti}w_N)=\frac{-14\,400}{T}+5.0 \tag{4}$$

$$\lg(0.07\times0.005)=\frac{-14\,400}{T}+5.0$$

$T_{ps}=1\,703$ K(1 430 ℃)

Nb(C,N)

$$\lg\left[w_{Nb}\left(w_C+\frac{12w_N}{14}\right)\right]=\frac{-6\,770}{T}+2.26 \tag{5}$$

$$\lg\left[0.04\times\left(0.08+\frac{12\times0.005}{14}\right)\right]=\frac{-6\,770}{T}+2.26$$

$T_{ps}=1\,431$ K(1 158 ℃)

NbC

$$\lg(w_{Nb}^{0.87}w_C)=\frac{-7\,530}{T}+3.11 \tag{6}$$

$$\lg(0.04^{0.87}\times0.08)=\frac{-7\,530}{T}+3.11$$

$T_{ps}=1\,388$ K(1 115 ℃)

TiC

$$\lg(w_{Ti}w_C)=\frac{-7\,000}{T}+2.75 \tag{7}$$

$$\lg(0.07\times0.08)=\frac{-7\,000}{T}+2.75$$

$T_{ps}=1\,399$ K(1 126 ℃)

2) Non-recrystallization temperature (T_{nr})

$$T_{nr}=867+464w_C+(6\,445w_{Nb}-644w_{Nb}^{1/2})+(732w_V-230w_V^{1/2})+890w_{Ti} \tag{8}$$

$$T_{nr}\approx867+37.12+257.8-128.8+62.3=1\,095.4\,℃$$

3) γ→α transformation temperature during cooling ($T_{A_{r3}}$) for $t=5$ mm:

$$T_{A_{r3}}=910-310w_C-80w_{Mn}+0.35(t-8) \tag{9}$$

$$T_{A_{r3}}=910-310\times0.08-80\times1.5+0.35\times(5-8)=910-24.8-120-1.05\approx764\ ℃$$

As mentioned, it is well established that the precipitation of Ti and Nb carbonitrides plays a very important role in controlling austenite grain growth during soaking and roughing operations and the precipitation of Nb carbonitrides retarding recrystallization at temperatures of finished controlled rolling operations[20]. It is well known that in the temperature range of interest, diffusion of carbon and nitrogen is some orders of magnitude faster than the diffusion of titanium and niobium. Therefore, Ti and Nb are expected to be the rate controlling elements[21-23].

3 Conclusions

Recently, the production and commercialization of UFF steels in their raw hot rolled state by TMCRP is a reality. Grain sizes range from 2 to 3 μm (ASTM $\overline{G}$ 14). The yield stresses are up to 700 MPa, and the uniform elongations are higher than 10%. These UFF steels are weldable owing to their low carbon content and they have low impact transition temperatures below 0 ℃. These steels are used in construction and in reinforcement parts for the automotive industry.

The achievement of these properties is the result of a careful control of chemical composition, including microalloying, the know-how acquired in the TMCRP, and giving a specific attention to the deformation sequences, austenite non-recrystallization temperatures, and γ→α allotropic transformation temperature during cooling.

These steels show ductility and forming capacity superior to the ones obtained by other techniques which, even worse, have not yet reached the industrial level, nor the commercial distribution.

The authors wish to thank the Research and Hot Coil Products Department of the ArcelorMittal in Asturias (Spain) Factories (formerly Ensidesa, CSI Planos, Aceralia and Arcelor). They also acknowledge Ms. Teresa Iglesias and Ms. Bertha Mendieta for their invaluable help in experimental work and text and figures revisions.

References:

[1] Eager T W. The Quiet Revolution in Materials Manufacturing and Production [J]. Journal of Metals, 1998, 50(4): 19.

[2] Advances in the Hot Rolling of Steels [J]. Ironmaking and Steelmaking, 2004, 31(1): 8.

[3] Perosanz J A. Steels: Physical Metallurgy. Selection and Design [M]. Madrid: CIE—Dossat, 2000 (in Spanish).

[4] Paxton H W. The Changing Scene in Steel [J]. Metallurgical Transactions, 1979, 10A(12): 1815.

[5] Pickering F B. Physical Metallurgy and the Design of Steels [M]. London: Applied Science Publishers, 1978.

[6] Vander Voort G F. Metallography: Principles and Practice [M]. Ohio: ASM International, 1999.

[7] Sellars C M. Quantitative Metallography for Master Course in Physical Metallurgy [R]. San Sebastián: CEIT de Guipúzcoa, 1981.

[8] Tsuji N, Ito Y, Saito Y, et al. Strength and Ductility of Ultrafine Grained Aluminum and Iron Produced by ARB and Annealing [J]. Scripta Materialia, 2002, 47(12): 893.

[9] Beladi H, Kelly G L, Hodgson P D. Ultrafine Grained Structure Formation in Steels Using Dynamic Strain Induced Transformation Processing [J]. International Materials Reviews, 2007, 52(1): 14.

[10] Furuhara T. Preface to the Special Issue on "Ultrafine Grained Steels" [J]. ISIJ International, 2008, 48(8): 1037.

[11] Okitsu Y, Takata N, Tsuji N. A New Route to Fabricate Ultrafine-Grained Structures in Carbon Steels Without Severe Plastic Deformation [J]. Scripta Materialia, 2009, 60(2): 76.

[12] Lesch C, Alvarez P, Bleck W, et al. Rapid Transformation Annealing: A Novel Method for Grain Refinement of Cold-Rolled Low-Carbon Steels [J]. Metallurgical and Material Transactions, 2007, 38A(9): 1882.

[13] Howe A. Ultrafine Grained Steels: Industrial Prospects [J]. Materials Science and Technology, 2000, 16(11/12): 1264.

[14] Leslie W C. The Physical Metallurgy of Steels [M]. New York: McGraw-Hill, International Book Company, 1981.

[15] Morrison W B, Miller R L. The Ductility of Ultra-Fine-Grain Alloys. Ultrafine-Grain Metals [M]. New York: Syracuse University Press, 1970.

[16] Bhadeshia H K D H. Bessemer Memorial Lecture: The Dimensions of Steel [J]. Ironmaking and Steelmaking, 2007, 34(3): 194.

[17] Backofen W A. Deformation Processing [J]. Metallurgical Transactions, 1973, 4B(12): 2679.

[18] Tamura I, Ouchi C, Tanaka T, Sekine H. Thermomechanical Processing of High Strength Low Alloy Steel [M]. London: Butterworths Ed, 1988.

[19] Perosanz J A. Materials Science and Engineering [M]. Madrid: Cie-Dossat, 2006 (in Spanish).

[20] Porter D A, Easterling K E, Sherif M Y. Phase Transformations in Metals and Alloys [M]. Boca Raton: CRC Press, 2009.

[21] Dutta B, Sellars C M. Effect of Composition and Process Variables on Nb(C, N) Precipitation in Niobium Microalloyed Austenite [J]. Materials Science and Technology, 1987, 3(3): 197.

[22] Dutta B, Palmiere E J, Sellars C M. Modelling the Kinetics of Strain Induced Precipitation in Nb Microalloyed Steels [J]. Acta Materialia, 2001, 49(5): 785.

[23] Liu W J, Jonas J J. Nucleation Kinetics of Ti Carbonitride in Microalloyed Austenite [J]. Metallurgical Transactions, 1989, 20A(4): 689.